Research, Society and Development, v. 11, n. 6, e13511628908, 2022
(CC BY 4.0) | ISSN 2525-3409 | DOI: http://dx.doi.org/10.33448/rsd-v11i6.28908

Live volume of conical stockpile reclaimed by gravity

Volume vivo de pilha cônica retomada por gravidade

Volumen vivo de pila cónica recuperada por gravedad

Received: 04/06/2022 | Reviewed: 04/13/2022 | Accept: 04/19/2022 | Published: 04/23/2022

Thiago Rios Ferreira
ORCID: https://orcid.org/0000-0001-8763-453X
Independent consultant on mining engineering, Brazil
E-mail: thiagorios84@gmail.com
José Aurélio Medeiros da Luz
ORCID: https://orcid.org/0000-0002-7952-2439
Federal University of Ouro Preto, Brazil
E-mail: jaurelio@ufop.edu.br
Matheus Henrique de Castro
ORCID: https://orcid.org/0000-0003-4422-1836
Petrobras S. A., Brazil
E-mail: matheus.h.castro@icloud.com

Abstract
Bulk solid stockpile reclaiming by gravity through bottom reclaimers at the base is a common method in the industry, as it is inexpensive, although it requires large plant floor areas. The complexity of actual particulate systems and the configuration of the recovery system often makes the quantitative prediction of dead volumes after recovery difficult, especially if historical or experimental data are not available. Incremental advances in design criteria and innovation can result in remarkable gains, due to the large amount of bulk materials currently handled. Research in this field, therefore, is still of importance. This article addresses the live volume fraction of conical stockpile recovered through underground hoppers and conveyor belt, comparing bench-scale empirical data with indirect measurements by drone-based aerial photogrammetry and mathematical modeling, via analytical geometry and computational simulation employing cellular automata. The results have shown excellent statistical adherence of the estimates both via photogrammetry and mathematical modeling.
Keywords: Gravity reclaim; Bulk solids handling; Cellular automata; Analytical geometry; Modeling teaching.

Resumo
A retomada gravitacional de pilhas de granéis através de retomadores na base é método comum na indústria, por ser barato, embora requeira grandes áreas de chão de fábrica. A complexidade dos sistemas particulados reais e da configuração do sistema de retomada torna, não raramente, a previsão quantitativa dos volumes mortos após a recuperação, difícil, máxime se dados históricos ou experimentais não forem disponíveis. Avanços incrementais nos critérios de projeto e em inovação podem resultar em ganhos notáveis, devidos à grande quantidade de granéis atualmente manuseados. A pesquisa neste campo, portanto, ainda se reveste de importância. Este artigo aborda a fração de volume vivo de pilha cônica retomada por meio de tremonha subterrânea e correia transportadora, comparando dados empíricos em escala de bancada, com medições indiretas por aerofotogrametria baseada em *drones* e modelagem matemática, por geometria analítica e por simulação computacional empregando autômatos celulares. Os resultados mostraram excelente aderência estatística das estimativas tanto via fotogrametria quanto por modelagem matemática.
Palavras-chave: Retomada gravitacional; Manuseio de granéis; Autômatos celulares; Geometria analítica; Ensino em modelagem.

Resumen
La recuperación gravitacional de las pilas de almacenaje de material a granel por medio de recuperadores de fondo es un método común en la industria porque es barato, aunque requiere grandes areas de la planta. La complejidad de los sistemas de partículas reales y la configuración del sistema de recuperación a menudo dificultan la predicción cuantitativa de los volúmenes muertos después de la recuperación, especialmente si no se dispone de datos históricos o experimentales. Los avances incrementales en los criterios de diseño y en la innovación pueden resultar en ganancias notables, debido a la gran cantidad de materiales a granel que se manejan actualmente. La investigación en este campo, por lo tanto, sigue siendo importante. Este artículo discute la fracción del volumen vivo de la pila cónica recuperada mediante tolva subterránea y cinta transportadora, comparando datos empíricos a escala de banco, con mediciones indirectas mediante aerofotogrametría basada en drones y modelación matemática, mediante geometría analítica y simulación computacional empleando autómatas celulares. Los resultados mostraron una excelente adherencia estadística de las estimaciones, tanto por fotogrametría, como por modelación matemática.

Palabras clave: Recuperación gravitacional; Manipuleo des sólidos a granel; Autómata celular; Geometría analítica; Enseñanza en modelado.

1. Introduction

The storage in big stockyards employing inferior reclaimer is quite used in the industry due to its convenience. However, some aspects of its use are more conditioned to empiricism than to the knowledge of the rheological behavior of the granular solids. One of the main problems is the determination of the useful pile's volume (Roberts, 2006; Luz & Peres, 1992), since part of the pile volume does not flow as a result of interparticle friction. A funicular surface occurs at the end of the flow of the so-called live volume. In general, this surface is modeled as conical, not infrequently with the inclusion of an axial conduit known as a "rathole". The situation worsens in the case of high stockpiles (sometimes up to 40 meters), which tends to lead to conservative design criteria, implying higher costs.

The correct estimation of the useful capacity of storage and regularization stockpiles becomes more difficult when it comes to multiple points of inferior reclaiming, especially in the case of non-symmetrical configurations (permanent or occasional) of the coordinates of the extraction points. To deal with this drawback, Luz and Perez (1992) have conceived a Monte Carlo-based system for simulation of generic positioning funicular surfaces, and adopting the simplification of circular reclaiming openings and conical surfaces with straight geratrices.

This work aimed at the comparison of estimation methods for the actual useful volume fraction of conical piles with lower reclaim. Mathematical modeling of the extraction funnel ultimate surface, which has been — generally and inappropriately — modeled as a conventional inverted cone, was also here performed, finding a funicular surface revolution with excellent topographical adherence to the experimental coordinates. In line with this modeling, the stockpile simulation was also performed using cellular automata-based algorithms. Completing the comparative study, an aerophotogrammetric survey of the experimental pile was carried out, using a small unmanned vehicle (drone), which demonstrated good positional accuracy. In order to perform this comparison, experiments to obtain constitutional parameters of silica sand, on a bench scale, were carried out.

2. Conceptual Framework: Parameters and Features

The experimental determination of granular media flow parameters is, in principle, a challenge. Firstly, it is due to the scarcity of standards for performing bench tests with granular materials. Secondly, because scale change does interfere directly with the material's flow behavior, hindering the calibration of models. It is also usually necessary, in parallel, mathematical modeling with satisfactory accuracy level that allows validation of parameters, thus avoiding the occurrence of problems, such as obstructions, segregation, etc. These parameters depend on factors such as particle size distribution, particle shape, chemical composition of the material, moisture, storage time, and temperature (Schulze, 2007).

Morphometry

The shape (and roughness) of the particles greatly influences their flowability. More rounded surfaces tend to have more flowability, while angular particles hinder the flow. Solid bulk particles usually have a wide variety of shape. Particle shape can be described, at least roughly, by the sphericity and roundness. The first one serves to demonstrate how close the particle is to a sphere of equivalent volume, while the second index is related to the degree of curvature of the corners, namely: vertices and edges (Suguio, 1973). According to Wadell (1935), sphericity is the relationship between the surface area of the equivalent sphere and the surface area of the particle. Its calculation is done by:

$$\psi = \frac{S_{eq}}{S_p} = \frac{\pi \times \left(d_{eq}\right)^2}{S_p} = \frac{\sqrt[3]{36 \times \pi \times V_p^2}}{S_p} \quad (1)$$

Where: ψ is the Wadell's sphericity; d_{eq} is the diameter of the equivalent sphere; V_p is the particle volume; and S_p is the actual surface area of the particle.

Occurrence of interstitial liquid (usually water) in unconsolidated granular media can substantially alter its properties. The size distribution of the material directly influences its behavior. Grains with a diameter smaller than 0.075 mm are more active in physical-chemical processes, and act in the expansion and contraction of the volume by varying the volume of water. However, grains with diameters greater than 0.075 mm to 2.0 mm have smaller specific surface areas and do not present significant physical-chemical activity. The interstitial liquid is more important in porosity and capillarity when the system is close to saturation (Das & Sobhan, 2014).

When it comes to porosity, Prado et al. (2022) have achieved good predictability in particulate systems that can be described by the Rosin–Rammler distribution, which can be expressed by:

$$Y_p = 1 - e^{\left[ln\left(\frac{1}{2}\right)\left(\frac{x}{x_{50}}\right)^q\right]} \quad (2)$$

Where: Y_p — mass fraction of particles of diameter smaller than x [–]; x — particle size [m]; x_{50} — median size [m]; q — sharpness parameter [–]. For such a system, with random packing, the porosity can be estimated by (Prado et al., 2022):

$$\varepsilon(q) = 0.2204 \times \left[1 - e^{-\left(\frac{q}{1.1419}\right)^{1.4411}}\right] + 0.1503 \quad (3)$$

Where: $\varepsilon(q)$ — volume bed porosity as a function of the sharpness index [–]. Equation (3) holds for spheroidal particles.

Dynamic angle of repose (α) of a granular material is the angle between the horizontal plane and the maximum slope of the surface resulting from a pile formed by free accumulation. It is appreciably affected by grain size and moisture. Discrepancies from the reference test, segregation of material, and variation of moisture over time may generate different values of angle of repose for the same material (Wadell, 1935).

Considering a previously dumped granular material, the subtended angle (β) between the horizontal plane and the maximum slope of the planar (unconfined) surface resulting from a reclaiming operation by a linear recovery system is called, here, static angle of repose, sometimes called "angle of reclaim" (Walker, 2009).

Powder flowability criteria

The bulk flowability is characterized by the ratio between unconfined tension (σ_c) and consolidation stress (σ_1), called the flow function, or Jenike's flow index (Bandeira et al., 2020), given by equation (4). The easier the flow, the smaller is the parameter ff_c (Figure 1).

$$ff_c = \frac{\sigma_1}{\sigma_c} \quad (4)$$

Unconfined and consolidation stresses are determinable by shear cell testing. This test consists of the application of shear force (applied at a constant speed) on the lid of a cylindrical chamber filled with the sample. The yield locus is used to measure the flowability parameters.

Figure 1 — Flowability as function of unconfined tension (σ_c) and consolidation stress (σ_1)

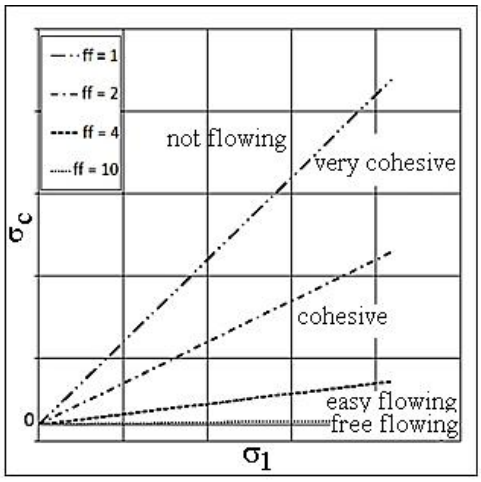

Source: Modified from Schulze (2008).

Hausner ratio and compressibility index

Hausner ratio (***HR***) and compressibility index (***CI***) are measures of gravity flowability of bulk solids and depend on the apparent density of the loose granular media, and on the ultimate density after sequential compaction (tapping) steps, reducing interparticle voids. For free-flowing materials, the density changes before and after compaction will be insignificant. High values correspond to low flowability (Carr, 1965). The Hausner index and the compressibility index are given respectively by equations (5) and (6):

$$HR = \frac{\rho_c}{\rho_a} \tag{5}$$

$$CI = \frac{(\rho_c - \rho_a)}{\rho_a} \times 100 \tag{6}$$

The parameter ρ_c is the ultimate density (tapped density) and ρ_a is the bulk density of the loose material (before tapping). For easy-flowing granular material has ***HR*** < 1.25 (***CI*** < 20 %); for fair-flowing material: 1.25 < ***HR*** < 1.40 (20 % < ***CI*** < 30 %); and for cohesive material: ***HR*** > 1.40 (***CI*** > 30 %).

Fraction of live volume

In the simplest case, a conical pile with incoherent material and a conical reclaim surface, in which the dimensions of the reclaimer/feeder are much smaller than the dimensions of the stockpile, the expression for the live volume fraction employing one central discharge opening for reclaiming is:

$$\varphi = \frac{[tg(\alpha)]^2}{[tg(\alpha) + tg(\beta)]^2} \tag{7}$$

The following figure (Figure 2) illustrates the mathematical idealization with circular central reclaimer with non-zero area and conical reclaim surface, a somewhat more complex case than the previous one. The center of the triorthogonal coordinate system is located at the floor level (***z*** = 0) and at the centroid of the discharge opening.

Figure 2 — Idealization of a conical stockpile, showing the theoretical axial reclaim cone for a reclaimer with circular cross section with center in (0;0;0).

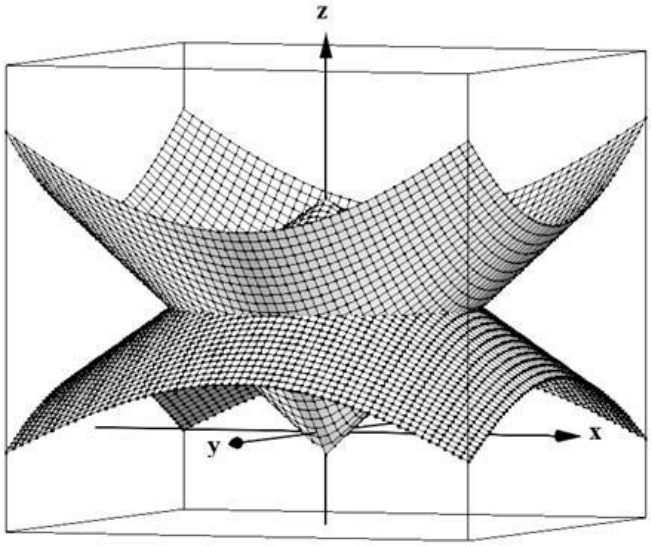

Source: Authors' own elaboration.

By adopting an axial circular discharge hole with the same area as the actual rectangular opening (as shown in Figure 2), one can - with moderate effort - deduce the fraction of useful volume, as a function of the equivalent radius (***r***) of the discharge hole, the pile diameter (***D***), the static and dynamic angles of repose (***β*** and ***α***, respectively). The fraction of useful or live volume can be calculated by the equation:

$$\varphi = \frac{8 \cdot \left\{ \left[\left(\frac{D}{2}\right) \cdot tg(\alpha) + r \cdot tg(\beta) \right] \cdot \left[\frac{D - 2 \cdot r}{2 \cdot \left(1 + \frac{tg(\beta)}{tg(\alpha)}\right)} + r \right]^2 - r^3 \cdot tg(\beta) \right\}}{D^3 \cdot tg(\alpha)} \quad (8)$$

From the model's premise, the equivalent radius is expressed as a function of the effective width (B_{ef}) and the length (***L***) of the actual rectangular discharge opening, resulting:

$$r = \sqrt{\frac{B_{ef} \times L}{\pi}} \quad (9)$$

In case of more than one reclaimer, there are a few plots that show the live volume percentages as a function of the number of reclaimers and/or the span between them, sometimes showing seemingly discrepant results (Allis Mineral Systems, 1994; Telsmith, 2011). Approach for complex reclaimers arrays was advocated by Luz and Peres (1992), based on Monte Carlo method.

Alternatively, erection and reclaim of bulk solid piles can easily be simulated using a two-dimensional model based on cellular automata, extrapolating to three dimensions, using the key concept of the Pappus-Guldinus theorem (Castro et al., 2021; Rautenberg & Probst, 2019).

3. Materials and Methods

Experimental setup: physical model

A platform was built for bench-scale experiments (Figure 3). It allowed the stacking and reclaiming of bulk solid

samples (siliceous sand), resulting piles with about 1.0 meter in diameter. The platform had a central rectangular aperture, under which was mounted the feed hopper that fed a conveyor belt, which was ultimately the cause of the granular material flow.

Figure 3 — Left: bench scale model of pile with reclaim opening and belt conveyor. Right: feed hopper sized (dimensions: x_1 = 80 mm; $x_2 = L$ = 0.200 m; $x_3 = B_{ef}$ = 0.060 m; equivalent radius: r = 0.0618 m).

Source: Authors' own elaboration.

The height of the hopper gate opening is the key factor for practical adjustment. It depends on the displacement, material density and the remainder geometry feature. Once the reclaiming flow in this section is considered plug flow (equal residence time for all particles at gate vicinity), in case of rectangular section (with side loading skirts) and flat belt conveyor, the flow rate equation can be presented as:

$$Q_v = \frac{dV}{dt} = \frac{dx \times A_c}{dt} = v \times A_c = v \times h \times B_{ef} = \frac{Q}{\rho_{ap}} \quad (10)$$

Where: dx is the elementary displacement in the direction of motion [m]; dt is the infinitesimal time interval [s]; dV is the volume that crosses the cross-sectional area in the time interval dt [m³]; A_c is the cross-sectional area to the movement [m]; h is the height of the outlet layer of the gate [m]; Q is the mass flow rate [kg/s]; Q_v is the reclaiming volumetric flow rate [m³/s]; B_{ef} is the effective width of the belt [m]; v is the velocity of displacement [m/s]; ρ_{ap} is the bulk (apparent) density of the granular material [kg/m³]. From the preceding equation one has:

$$h = \frac{Q}{B_{ef} \times v \times \rho_{ap}} \quad (11)$$

In case of a trapezoidal cross section of the material on the belt, with the smaller base (top) having dimension b [m], the cross-sectional area of the stream tube would be:

$$A_c = \left(b + \frac{h}{tg(\beta_{sur})}\right) \times h \quad (12)$$

Where β_{sur} is the angle of surcharge. Applying this formula in the preceding equation, the volumetric flow rate can be expressed by a second-degree equation with respect to height:

$$Q_v = \frac{Q}{\rho_{ap}} = v \times \left(b + \frac{h}{tg(\beta_{sur})}\right) \times h \times \rho_{ap} \quad (13)$$

Good engineering practice recommends that the slope of the hopper chute should always be higher than 60 °, and it is

therefore reasonable to adopt 75°. In operation, it is usually recommended that its speed should also not exceed 0.5 m/s. Another usual design criterion is that, at the exit from the hopper to the belt, the width of the reclaim mouth should be at least 2.5 times larger than the particle top size.

The size and shape of the opening depends directly on the discharge flow rate and the flow function for a given material. According Jenike (1961), the discharge opening dimension should be the ratio between the unconstrained tension and the material density.

In the experiments the granular material was dumped over the center of the platform from height of 0.5 m. The adjusted flow rate for the reclaim system was $\boldsymbol{Q}$ = 0.200 kg/s, using slot of the slide gate $\boldsymbol{h}$ = 0.06 m and effective width $\boldsymbol{B_{ef}}$ = 0.06 m. The belt speed resulted equal to 3.97 cm/s.

For the validity of the experiment, the material to be used must be or represent those applied in the industry, besides having a good flow condition. In order to meet these requirements, two sand samples from construction sector industry were used for conducting the experiments. Fine sand and medium sized sand commercial specifications were used.

Live volume through aerial photogrammetry

At this stage of the work the calculation of the live volume was performed using the technique of digital mapping by aerial survey with drone (from Aeromine Company). The use of drones and a remotely piloted aircraft (RPA) has been advocated to improve productivity and safety in industrial areas (Soares Jr. et al., 2021; Silva Neto et al., 2021). Photographic georeferencing was not effective due to the reduced scale of the tests. However, it was offset by the use of checkpoints intentionally inserted in the experiment scene. Drone flight height setpoint was 3.55 m. The statistical parameters of altimetry have shown good control performance. The actual average flight height was 3.5475 m, with standard deviation of 0.0035 m, and Pearson's coefficient of variation of 0.0998 %. This is in line with achievements of Candido et al (2018), which demonstrate high spatial resolution of aerial photogrammetry by unmanned aerial vehicles.

Modelling by analytical geometry

The extraction cone shown in Figure 2, commonly does not properly represent the reclaim surface, because of the common occurrence of "ratholes", a phenomenon that has been studied, for instance, by Roberts (Roberts, 2005; Roberts, 2006). Within this context, surfaces of revolution that could take into account the existence of these axial channels (Dornelas et al., 2021) were prospected here. In short, several generating lines that could result funnel-like surfaces of revolution were sought. After careful geometrical research, generating lines (starting in the ***xz*** plane) of type bellow were adopted:

$$z(x') = \left[\left(\frac{x'}{r}\right)^n - \left(\frac{x'}{r}\right)^m\right]^{\frac{1}{n}} \times r \times tg(\beta) \tag{14}$$

Parameters $\boldsymbol{n}$ and $\boldsymbol{m}$ are even (in order to get mirror symmetry) and $\boldsymbol{n} > \boldsymbol{m}$. Here, $\boldsymbol{x'}$ is the abscissa, restricted to the vertical plane ***xz***. The funnel-like ("funicular") revolution curve around the ***z***-axis will therefore be given by:

$$z = f(x') = f\left(\sqrt{x^2 + y^2}\right) = \left[\left(\frac{\sqrt{x^2 + y^2}}{r}\right)^n - \left(\frac{\sqrt{x^2 + y^2}}{r}\right)^m\right]^{\frac{1}{n}} \times r \times tg(\beta) \tag{15}$$

It should be noted that, as $\boldsymbol{n}$ is greater than $\boldsymbol{m}$, when $\boldsymbol{x}$ assumes large values (that is, when it moves away from the confinement condition), the surface tends to a cone with wall slope angle equal to the asymptotic value ($\boldsymbol{\beta}$ is the angle of static friction, or angle of reclaim, in a flat slope). The following figure shows the profile of two generating lines, with promising

exponents: ***m*** = 2, and ***n*** = 4 or, alternatively, ***n*** = 6.

Figure 4 — Two generating lines for funnel-like reclaim surface with β = 48.46º; r = 0.0618 m; m = 2 (curve 1: ***n*** = 6; curve 2: ***n*** = 4).

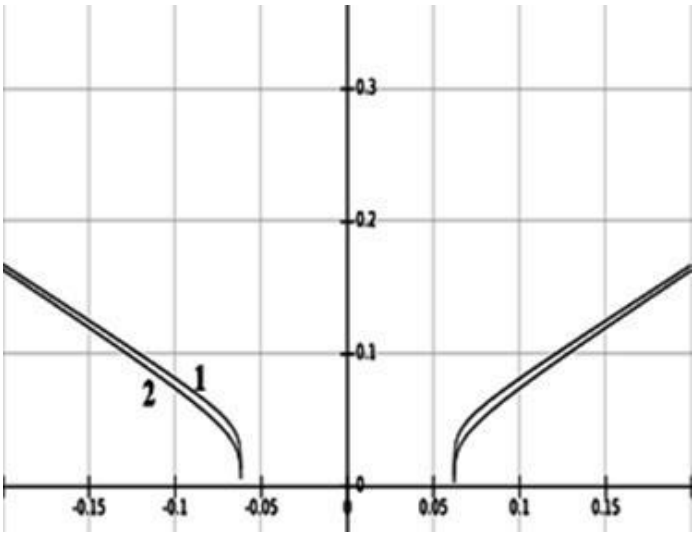

Source: Authors' own elaboration.

In order to calculate $\boldsymbol{\beta}$ (asymptotic), the average value of the tilt angle of the cone ($\boldsymbol{\beta_{cone}}$) with the same area as the opening for basal reclaim — and with the same (3D) curve of intersection with the pile cone — was initially calculated, from a pile's photographic top view after the end of a reclaiming operation. Thereafter, using analytical geometry, the value of the asymptotic slope angle of the funnel-like surface was calculated. The corresponding equation was:

$$\beta = arctg\left[\frac{(x_i^{'} - r) \times tg(\beta_{cone})}{r \times \sqrt[n]{\left(\frac{x_i^{'}}{r}\right)^n - \left(\frac{x_i^{'}}{r}\right)^m}}\right] \quad (16)$$

The following figure illustrates the geometric constraints (at intersection point I), using typical numerical values for the system under study (fine sand).

In order to calculate the live volume of the modeled cell, one can apply the Pappus-Guldinus theorem, which is expressed by:

$$V = \theta \times x_c \times A_c \quad (17)$$

Where: ***V*** is the volume generated by the revolution of the generating line; $\boldsymbol{\theta}$ is the angle of revolution executed around the axis; $\boldsymbol{x_c}$ is the distance from the centroid of the plane figure to the axis of revolution; $\boldsymbol{A_c}$ is the area of the rotating flat figure, i. e.: area between the curve (3) of Figure 5 and the line $\boldsymbol{x} = \boldsymbol{r}$, plus the rectangle between the vertical lines $\boldsymbol{x} = 0$**,** and $\boldsymbol{x} = \boldsymbol{r}$, with the average height of the crest (point of intersection point ***I***). In the present case: $\boldsymbol{\theta} = 2\boldsymbol{\pi}$.

Figure 5 — Generating lines: cone of pile (1), apparent reclaim cone (2) and funnel-like curve (3).

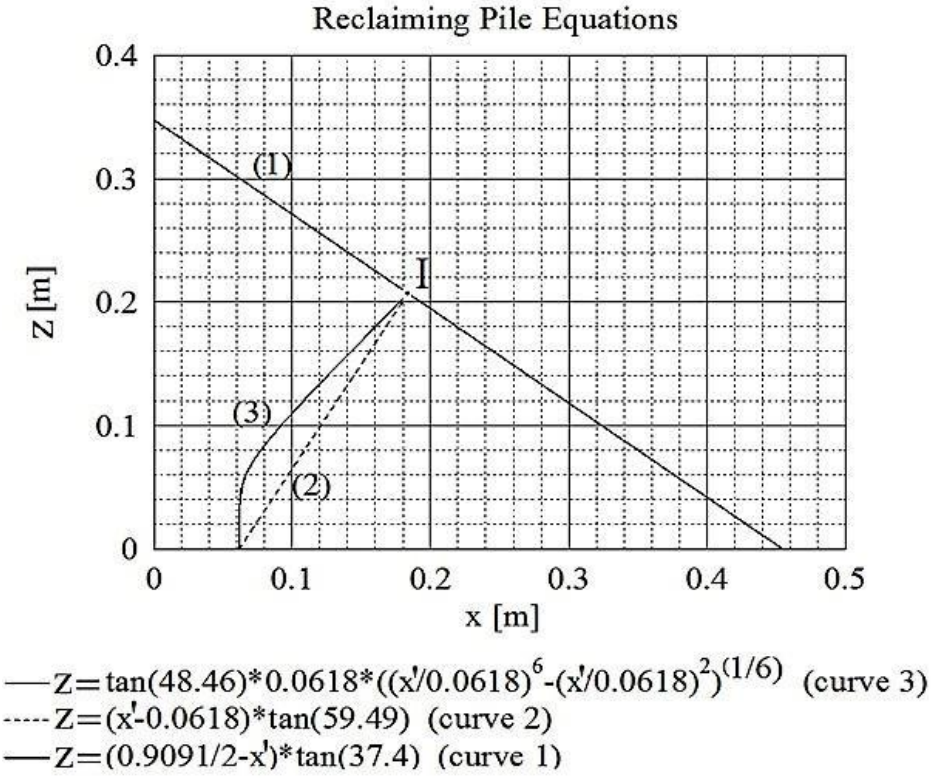

Source: Authors' own elaboration.

The area comprised between curve (3) of Figure 5 and $\boldsymbol{x} = \boldsymbol{r}$ can be easily obtained by using a numerical integration method in a spreadsheet, as well as the abscissa of its centroid, which is expressed by:

$$x_c = \frac{1}{A_c}\int_S x \times dS \tag{18}$$

In the present work, 500 points of integration were used employing the trapezoidal method, and the results have coincided with the values obtained by the *EasyPlot*® software (a statistical package from Spiral Software).

Modelling by cellular automata

This modeling was performed following the method preconized by Castro et al. (2021). In this type of stockpile model, a ternary composition of grain sizes was used, the smaller grain being represented by 1 pixel, or 1 mesh cell, and the larger grain represented by 9 pixels (3 x 3 pixels), or nine mesh cells. In view of this, the effects of segregation are pronounced, as the pile is built, causing the grains to 'fall' from the pile axis.

The construction of the pile ends when its base meets one of the side limits of the mesh of cellular automata. After this, the simulation of the reclaiming process at its base is started; This is done by 'eliminating' the grains randomly located at the base and around the axis, according to a Gaussian distribution, and by letting the adjacent grains 'flow' down, or similarly, by making the voids generated at the base, flow up the stack.

4. Results and Discussion

Experiments

As a previous step, characterization was performed and the results for the two samples are given in the Table 1.

Table 1 — Samples properties datasheet.

Sand type	*Particle diameter, d_p*	*Bulk density*	*Moisture*	*Angle of repose*	*Hausner ratio*	*Compressibility index*
Medium	0.6 to 0.2 mm	1380.0 kg/m³	1.9 %	34º	1.04	4.4 %
Fine	0.2 to 0.06 mm	1420.0 kg/m³	3.1 %	39 º	1.09	9.8 %

Source: Authors' own elaboration.

The experimental results for stockpile models using the two sand specifications are summarized in Table 2, together with their descriptive statistics.

Table 2 — Experiments results and their statistical variability.

Property	***Fine sand***	***Medium sand***
Live volume fraction average	17.74 %	17.79 %
Sample standard deviation of live volume fraction	0.0037 %	0.0046 %
Pearson's coeficiente of variation	2.08 %	2.71 %
Uncertainty (percentage points) of the live volume fraction (by Student's t-test)	0.26 %	0.35 %

Source: Authors' own elaboration.

The fraction of live volume obtained by the mass balance was compared with the value presented in Faço's Manual of Crushing (Allis Mineral Systems, 1994), which deals with abacuses of prediction of stockpile's live fraction for reclaim systems.

Figure 6 — Pile configuration, before and after a reclaiming test.

Source: Authors' own elaboration.

Live volume through aerial photogrammetry

The volumetric analysis of the fine sand pile, after image treatment for conversion of the information from pixels to cubic meters, has gotten the following results: initial pile volume was 0.07333194 m³, the remaining volume after reclaim was

0.06035318 m³ resulting a fraction of useful volume of 17.69 % (Figure 7). The same procedure was performed for the experiment using medium sized sand as material. The initial volume was 0.06853452 m³, the remaining volume after recovery was equal to 0.05674558 m³, resulting in 17.20 % for useful volume fraction.

Figure 7 — Right: processed image of the medium sand pile after reclaim. Left: draft displaying radial dimensions to calculate the average static angle of repose.

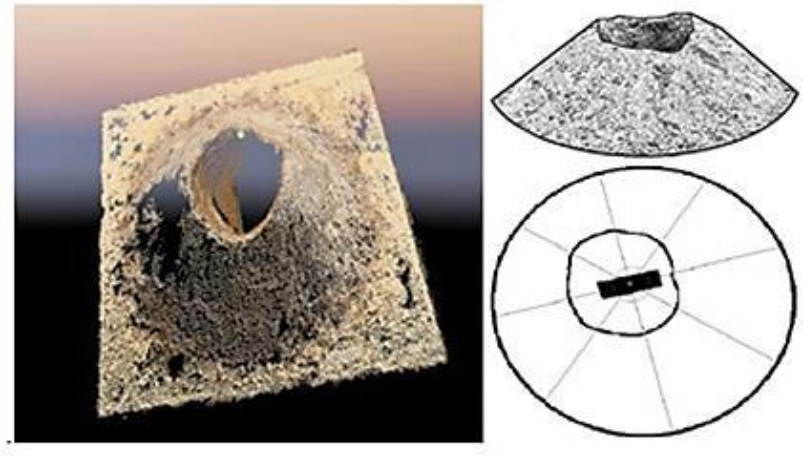

Source: Authors' own elaboration.

Modelling by analytical geometry

The measurement of the horizontal projection of the extraction crater crest allowed the estimation of the experimental general static angle of repose: β_{cone} = 59.49º (average of eight radial values, as shown in figure 7). The application of this average in Equation 16 has returned an average static angle of repose (asymptotical): β = 48.46º.

The best statistical adherence to the experiments was obtained with the exponent values: m = 2 and n = 6 of funicular crater following Equation 15. This mathematical model can be seen in Figure 8.

Figure 8 — Funnel-like reclaim surface, with m = 6; n = 6; - 0.3 m ≤ x ≤ + 3.0 m; - 0.3 m ≤ y ≤ + 3.0 m; - 0.05 m ≤ z ≤ + 0.55 m (image powered by Google Chrome).

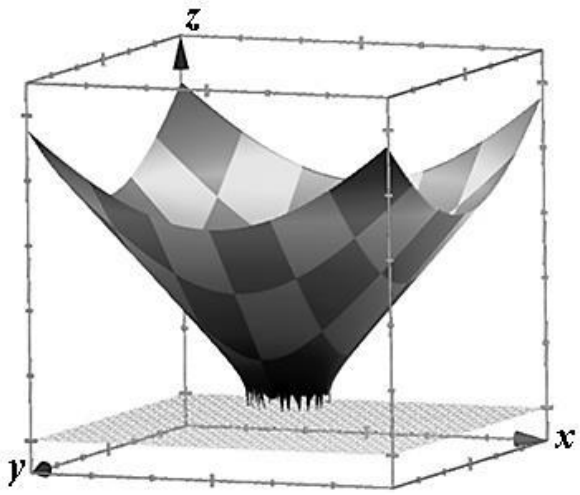

Source: Authors' own elaboration.

The fraction of useful volume calculated for conical reclaim was close to the empirical values, but with a higher value: 20.72 %. Keeping the same parameters, the fraction of live area in the cross-section of the system accounted for 48.53 %.

In turn, the fraction of useful volume calculated for recovery with funicular surface was very close to the empirical value, being equal to 17.35 %.

Modelling by cellular automata

In the following model, the cross-sectional area covered by the small grains (lighter shade), and by the large grains (darker shade), is the same, so that the volumetric ratio of each size range in the feed during the simulation of the stacking (pile formation) is 50 %. However, the proportions during the reclaim do vary, by the effects of size segregation.

Figure 9 —Two-dimensional stockpile modeled via cellular automata and resulting dead cross-sectional area.

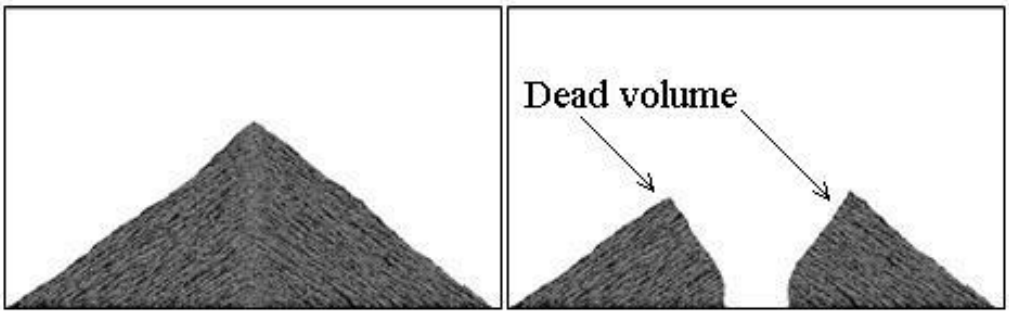

Source: Authors' own elaboration.

The angle of repose of the model arises from the composition of fine and coarse particles. In this simulation, the maximum allowed angle for fine particles and medium sized particles is 45º and for the coarse particles 52º. The value obtained for the resulting angle of repose was 37.3°.

During reclaim, the model constraints have imposed a limitation to the gravity flow of the particles, with descending inclined movement being up to 45º, but, as observed, stratification appears to play a resistance to flow, increasing the angle of repose to 56°.

In the model of Figure 9, the 2-D stockpile consists of 56,748 grains of size 1, 13,874 grains of size 2, and 6,177 grains of size 3, representing a total volume of 56,748 + 4 × 13,874 + 9 × 6,117 = 167,297. The 'dead' area represented in Figure 9 has a total value of 29,966 + 4 × 7,863 + 9 × 3,844 = 96,014. This results in a fraction of useful cross-sectional area equal to 42.6 %. The Pappus-Guldinus theorem must be used to calculate the value of the useful volume, assuming the surface of revolution, with the **z**-axis of rotation (Gual-Arnau & Miquel, 2006).

The specular symmetry of the generated model is not mathematically perfect. Then, the Pappus-Guldinus theorem was integrated so that the values of the areas have undergone a linear modification from the lowest value to the highest value, as the angle of rotation increased (from 0 to π). The corresponding values of the radii of rotation (from the axis of rotation to the areas centroids) also have suffered the same linear variation. The volume after the "revolution" was calculated by:

$$V = 2\int_0^{\pi} \bar{d}(\theta)\, A_c(\theta) d\theta \quad (19)$$

Where:

$$A_c(\theta) = A_{cL} + \frac{(A_{cR} - A_{cL}) \times \theta}{\pi} \begin{cases} se\ A_{cR} > A_{cL} \\ para\ \theta \in [0, \pi] \end{cases} \quad (20)$$

$$\bar{d}(\theta) = d_L + \frac{(d_R - d_L) \times \theta}{\pi} \begin{cases} se\ d_R > d_L \\ para\ \theta \in [0, \pi] \end{cases} \quad (21)$$

Here: $\boldsymbol{A_{cL}}$ — area of the left part of the pile [m²]; $\boldsymbol{A_{cR}}$ — area of the right part of the pile [m²]; $\boldsymbol{d_L}$ — distance from the centroid of the left part of the pile [m]; $\boldsymbol{d_R}$ — distance from the centroid of the right part of the pile [m].

Solving this integral, the equation for the three-dimensional stockpile volume is:

$$V = 2\pi \times \left(\frac{A_{cL} \cdot d_L}{3} + \frac{A_{cL} \cdot d_R}{6} + \frac{A_{cR} \cdot d_L}{6} + \frac{A_{cR} \cdot d_R}{3}\right) \quad (22)$$

As shown in Figures 10 and 11, the centroid on each side of the axis closely approximates the intersection of medians (blue) of approximate triangle (red) on each side.

Figure 10 — Approximation between the centroids of the pile's sides (before reclaim), with the intersection of medians (in blue) of the triangles (in red).

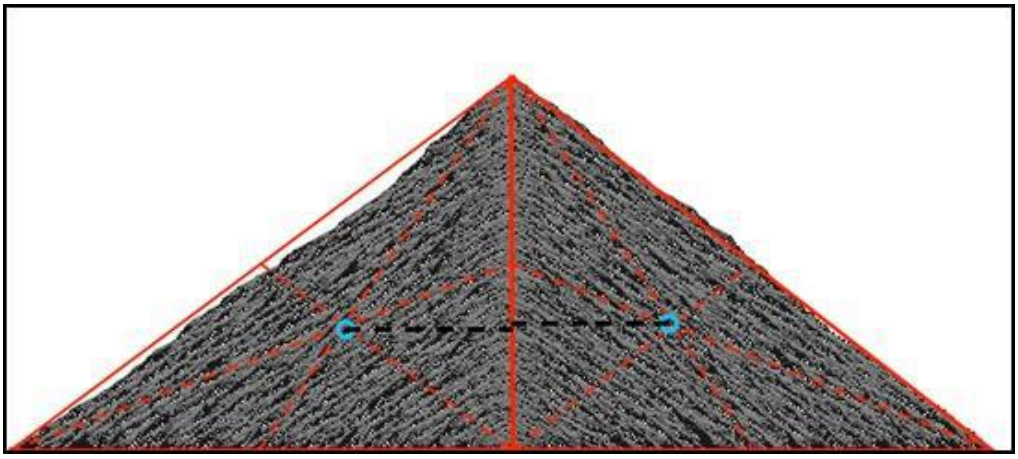

Source: Authors' own elaboration.

Figure 11 — Approximation between the centroids of the pile's remaining sides (after reclaim), with the intersection of medians (in blue) of the triangles (in red).

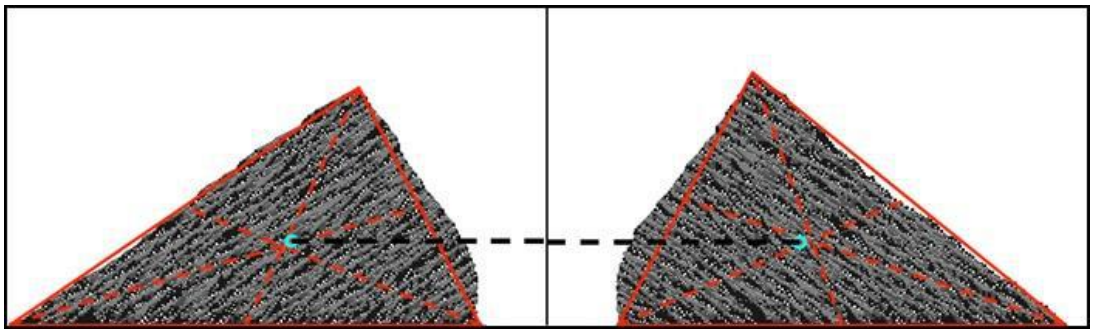

Source: Authors' own elaboration.

Therefore, the volume for the initial conical pile (from Figure 10) was that volume that would correspond to 84,119,346 active pixels; whereas, after the reclaiming operation, the simulated residual volume (from Figure 11) has corresponded to

70,716,172 pixels. These numbers entail a fraction of the estimated useful volume of 15.60 %.

It should be noted that the three-dimensional (and non-prismatic) pile configuration leads to a considerable difference between the fraction of live area (apparent in a given cross section) and the effective fraction of useful or live volume. Considering the cross-sectional area in the plane of symmetry, the fraction of live area by analytical modelling using conical geometry has resulted in 48.53%, while, by simulation through cellular automata, the fraction of live area was equal to 42.60%.

5. Conclusion

The dynamic volume quantification with the use of small-scale unmanned aerial vehicles (drones) proved to be fully reliable, and the experimental measurements of the live volume fraction, by weighing the stacked material and the remaining material after reclaiming operation, stayed at 17.74 % ± 0.26 % for fine sand and, on the other hand, 17.79 % ± 0.35 % for medium sand sample. The corresponding estimates, using drones, resulted in 17.69 % and 17.20 %, respectively. As far as the method employing analytical geometry is concerned, the value was very close to the estimate by aerial photogrammetry, resulting the value of 17.35%.

Regarding the simulation by cellular automata, the results were satisfactory under the studied conditions, since the estimated useful volume fraction was 15.60 %. Part of the difference for less is probably due to the greater internal porosity of the stack, by virtue of the algorithm used.

As a final consideration, it is interesting, in the future, to expand the scope of the present investigation, taking into account multiple reclaiming hoppers and other geometric configurations of stockpiles (radial piles and longitudinal ones). Undoubtedly, these are promising topics for the continuity of this kind of research, which will result in useful future publications.

Acknowledgments

The authors are thankful to Brazilian Council for Technological and Scientific Development (CNPq), Foundation for Research Support of the State of Minas Gerais (FAPEMIG), Brazilian Federal Agency for Support and Evaluation of Graduate Education (CAPES), and Vale Institute of Technology (ITV) for their financial support. They also are grateful to Depósito Interbrasil, Aerotech Group – division Aeromine, Madeireira Gouvêa & Funzo and Mangia Artinox for material and logistic support. The authors also take the opportunity to declare that there is no conflict of interest regarding the publication of this article.

References

Allis Mineral Systems – Fábrica De Aço Paulista (1994). *Manual de britagem Faço*. (5a ed.), Allis Mineral Systems.

Bandeira, D. J. A., Nascimento, J. J. da S., & Nascimento, J. W. B. do. (2020). Análise do fluxo de ração avícola em silos verticais esbeltos com insert de cone invertido. *Research, Society and Development*, 9(11), e63091110369. https://doi.org/10.33448/rsd-v9i11.10369

Cândido, A. K., Paranhos Filho, A. C., Marcato Júnior, J., Silva, N. M., Haupenthal, M. R., Oliveira, J. R., Marini, L. B., & Toledo, A. M. (2018). Positional accuracy of aerophotogrammetric survey in the Pantanal derived from UAV. *Geociências*, *37*(1), 137–146. https://doi.org/10.5016/geociencias.v37i1.11291

Carr, R. L. (1965). Evaluating flow properties of solids. *Chemical Engineering*; 72, 163-168.

Castro, M. H. de, Luz, J. A. da, & Milhomem, F. de O. (2022). Cellular automaton-based simulation of bulk stacking and recovery. *Journal of Materials Research and Technology*, *16*, 263–275. https://doi.org/10.1016/j.jmrt.2021.11.127

Das, B. M. & Sobhan, K. (2014) *Principles of Geotechnical Engineering* (8th ed.). Stamford: Cengage Learning.

Dornelas, K. C., Ayres, G. D. J.., & Nascimento, J. W. B. do. (2021). Emprego de inserts em silos metálicos: revisão sobre o padrão de fluxo dos produtos e distribuição das cargas na estrutura. *Research, Society and Development*, 10(4), e55710414580. https://doi.org/10.33448/rsd-v10i4.14580

Gual-Arnau, X., & Miquel, V. L. (2006). Pappus-Guldin theorems for weighted motions. *Bulletin of The Belgian Mathematical Society-Simon Stevin*, 13, 123–137.

Jenike, A. W. (1961). Gravity flow of bulk solids. *Bulletin of the University of Utah*, Salt Lake City, 52(29).

Luz, J. A. M. da, & Peres, A. E. C. (1992, setembro). Cálculo de volume útil de pilhas de granéis pelo método de Monte Carlo simples. In V. S. T. Ciminelli & M. J. G. Salum (Eds.): *Anais do III Encontro do Hemisfério Sul sobre Tecnologia Mineral — São Lourenço, MG*. ABTM.

Prado, D. R., Luz, J. A. M. da, Milhomem, F. de O., & Paracampos, M. P. S. (2022). On bed porosity of multisized spheroidal particles. *Brazilian Journal of Development*, 8(2), 14217–14237. https://doi.org/10.34117/bjdv8n2-378

Rautenberg, R. R., & Probst, R. W. (2019). Os teoremas de Pappus para os sólidos de revolução. *Revista Transmutare*, Curitiba, 4, e1912312, 1–59.

Roberts, A. W. (2005). Characterization for hopper and stockpile design. In D. Mcglinchey (Ed.). *Characterization of Bulk Solids. Oxford: Blackwell-CRC*. 2005. pp.:85 – 131.

Roberts, A. W. (2006). An Historical Overview and Current Developments; *Bulk solids handling*, Clausthal-Zellerfeld, 26(6), 392-419.

Schulze, D. (2008). *Powder and bulk solids – Behavior, characterization, storage and flow*. Berlim: Springer. 517 p.

Silva Neto, J. O., Sasaki, R. S., & Alvarenga, C. B. de. (2021). Aeronave Remotamente Pilotada (RPA) para aplicação de agrotóxico. *Research, Society and Development*, 10(12), e293101220573. https://doi.org/10.33448/rsd-v10i12.20573

Soares Jr., G., Satyro, W., Bonilla, S., Contador, J., Barbosa, A., & Monken, S. et al. (2021). Construction 4.0: Industry 4.0 enabling technologies applied to improve workplace safety in construction. *Research, Society and Development*, 10(12), 1–18.

Suguio, K. (1973). *Introdução à sedimentologia*. Edgard Blücher. 317 p.

Telsmith. (2011). *Mineral Processing Handbook (13th edition)*. Mequon: Telsmith. 220 p.

Wadell, H. (1935). Volume, shape and roundness of quartz particles; *Journal of geology*, Chicago, 43(3), 250-280.

Walker, Harold A. (2009). *Patent US20100272543 - Bulk material storage and reclaim system*. Google Books. https://www.google.com/patents/US20100272543.